

Fiber Parametric Amplifiers for Wavelength Band Conversion

Mohammed N. Islam and Özdal Boyraz, *Student Member, IEEE*

Invited Paper

Abstract—By using a loop configuration formed by a polarization beam splitter, we experimentally demonstrate that the existing wavelength-division multiplexing (WDM) sources in *C*-band can be wavelength converted to the *S*-band with low polarization sensitivity and low crosstalk. Using a fiber parametric amplifier as a band converter, we achieve experimentally <0.65 -dB polarization sensitivity and >4.7 -dB conversion efficiency over 30-nm conversion bandwidth in 315 m of fiber. Compared to the conventional straight fiber wavelength conversion scheme, a more than 2-dB improvement in polarization sensitivity is measured. In addition to the polarization insensitivity, channel crosstalk is measured to be <-27 dB in 315 m of high nonlinearity fiber. In a detailed experimental study, the pattern of crosstalk in longer fiber lengths and the coupling between the polarization sensitivity and crosstalk are measured. For example, with a 430-m fiber length, we measure the degradation in polarization sensitivity to be ~ 4 dB for 12-dB increased signal power. The experimental results are also confirmed by theoretical calculations. Moreover, in a 32 channels systems simulation, the signal-to-noise ratio (SNR) of the converted signals after 800-km propagation is calculated to be only 0.8-dB degraded compared to using laser diodes with the same initial SNR values. Furthermore, we calculate the effect of pump noise and show that the relative intensity noise of the pump is transferred to the converted signals with an additional 8-dB/Hz degradation.

Index Terms—Broad-band amplifiers, crosstalk, nonlinear optics, optical fiber amplifiers, optical parametric amplifiers, optical fiber communication, optical fiber polarization, optical propagation in nonlinear media, optical transmitters, parametric amplifiers, polarization sensitivity, wavelength-division multiplexing, wavelength conversion.

I. INTRODUCTION

FIBER PARAMETRIC amplifiers can be used to convert simultaneously a set of wavelengths to a new set of wavelengths, which are a mirror image of the original. A band converter of this sort can fulfill a number of unique functions in telecommunications networks. For example, in a protection switching or restoration mode, the band converter can take an existing band of wavelengths on a damaged link and transfer it to a new band of wavelengths on an already used fiber. Alternately, to reduce capital expenses and operational

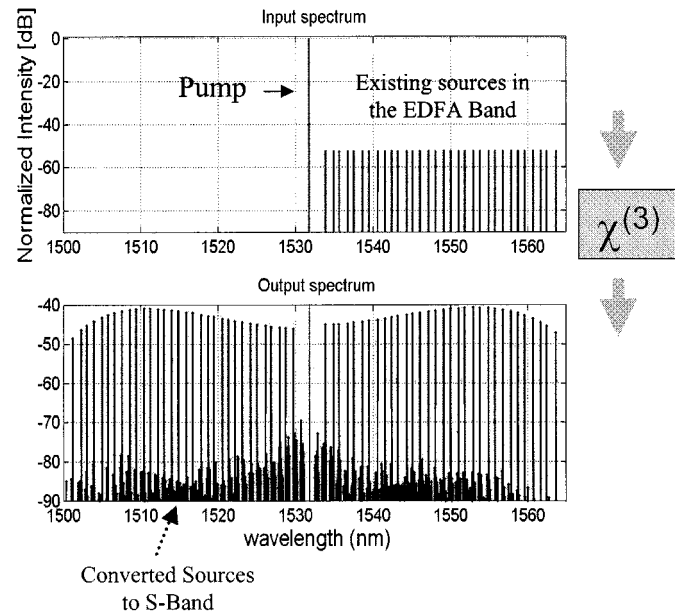


Fig. 1. Illustration of *S*-band source generation by wavelength conversion. By using a single pump laser to utilize modulation instability, the existing sources in *C*-band can be converted to *S*-band. The mirror image of the sources in the *C*-band is generated in the *S*-band.

expenses through fewer part numbers, it may be desirable to only stock a fixed number of WDM transmitters, such as only in the conventional *C*-band. Then, new transmitters in the surrounding bands—such as the short-wavelength *S*-band or long-wavelength *L*-band—can be made by using the existing transmitters and band shifting them to either the *S*- or *L*-band. However, a band converter for any of these telecommunications applications must be polarization insensitive with low crosstalk between WDM channels.

An attractive method of implementing the band conversion process is based on the modulation instability (MI) effect in the fiber. MI is a four-photon process, where two photons from the pump laser and one photon from the signal interact and generate one photon in signal wavelength and one in conjugate, which is the image of the signal. Fig. 1 shows the basic idea behind the process. Starting with high-power pump laser near low power signal channels stimulates the third-order nonlinear $\chi^{(3)}$ effects in fiber. The MI process is the special case of third-order nonlinear effect when the pump and signal wavelengths are near zero dispersion wavelength of the fiber and both at anomalous

Manuscript received January 31, 2002; revised April 2, 2002. This work was supported by DARPA at the University of Michigan.

M. N. Islam is with Xtera Communications, Inc., Allen, TX 75013 USA. He is on leave-of-absence from the EECS Department, University of Michigan, Ann Arbor, MI 48109 USA.

Ö. Boyraz is with Xtera Communications, Inc., Allen, TX 75013 USA.

Publisher Item Identifier S 1077-260X(02)05900-2.

dispersion regime. The conversion bandwidth, however, is determined by the pump power and the dispersion properties of the fiber, which determines the phase-matching condition. By choosing high nonlinearity fibers and a pump laser near the zero dispersion wavelength of the fiber while maintaining a relatively low dispersion value at the signal band, the entire *C*-band can be converted to the *S*-band in low dispersion fibers. However, the efficiency of the MI depends on the relative polarizations of the signal-and-pump lasers. This polarization sensitivity may cause amplitude fluctuations at the output due to random changes in the polarizations states of the incoming signals. Moreover, as the signal and the pump power increase, non-degenerate four-wave mixing (FWM) generates additional harmonics. If multiple wavelengths are converted, then these new harmonics may cause crosstalk between nearby channels.

By using a loop configuration formed by a polarization beam splitter and a fiber of optimized length, a polarization sensitivity of less than 0.65 dB over 30 nm and crosstalk less than -27 dB can be achieved. The aim is to use two pump beams to convert each polarization state separately. By using a polarization beam splitter (PBS), two polarization states of the incoming signal can be separated and combined with one of the pump beams. By using the loop configuration, the same fiber is utilized to eliminate differences in gain values. The interactions between the orthogonal pump lasers can be minimized by counterpropagation around the loop. However, a length optimization is required to optimize the crosstalk value. Specifically, since the strength of the harmonic is increased with fiber length, the fiber length should be cut before the harmonics reach a power level that causes a significant crosstalk. Additionally, using short fiber lengths for wavelength conversion can minimize the coupling between the polarization sensitivity and the crosstalk, even though the shorter fiber results in lower conversion efficiency.

The outline of this paper is as follows. The next section provides the background of various approaches on wavelength conversion. Then, band conversion in straight fibers is demonstrated in three different fiber lengths with special focus on the crosstalk measurements. The polarization-insensitive wavelength conversion in high-nonlinearity dispersion-shifted (HNL-DS) fiber in a loop configuration will be presented in Section IV. Theory of wavelength conversion and verifications of the experimental results will be given in Section V. The system performance based on 32 channels continuous-wave (CW) propagation through 800 km and the effect of pump noise on converted signals will be discussed in Section VI. Section VII will have a brief discussion of the experimental results, followed by a summary of the paper in Section VIII.

II. BACKGROUND

There are several experimental and theoretical researches conducted on parametric amplifiers and wavelength converters to develop new amplifiers and convert existing sources to improve the wavelength efficiency of WDM networks by allowing wavelength reuse [1]–[3]. Specifically, several groups within last decade have investigated the different aspects of conversion of existing laser sources to different wavelengths

and amplification of signals in optical fibers. One aspect of the research focuses on the gain flatness of the amplifiers and gain ripple [4], [5]. The other aspect of the research focuses on the high conversion efficiency and large conversion bandwidth of parametric amplifiers and wavelength converters [6]–[9]. In addition, there has been several papers presented on generation of new sources by utilizing the parametric process in fibers and semiconductor optical amplifiers [10]. However, the intrinsic polarization sensitivity and channel crosstalk problems, as pointed out in these experiments, limit the applications [1], [11].

The early polarization works generally focused on the conversion efficiency of FWM for different polarization states [11]. In later experiments, there are several approaches presented to achieve polarization-insensitive wavelength conversion both in semiconductor optical amplifiers (SOA) and in dispersion-shifted fibers (DSF) with low conversion efficiencies [12]–[16]. Orthogonally polarized pump sources to achieve polarization diversity pumping is the most commonly used technique in these experiments to achieve low polarization sensitivity [14], [15]. For example, in one of the early experiments, Jopson *et al.* implemented a wavelength converter with >1-dB polarization sensitivity in 25-km DSF by using two orthogonally polarized pump signals symmetrically located around the zero-dispersion wavelength of DSF [12]. In a later experiment, the polarization sensitivity of the similar setup is reduced to 0.3 dB at certain wavelengths by using tunable pump lasers to optimize pump position in a different 13-km DSF [13]. Likewise, single frequency conversion with as low as 0.5-dB polarization sensitivity has been demonstrated by using two pump lasers at different wavelengths and orthogonal polarizations [14]. Recently, there has been field transmission of 40 Gb/s with midspan inversion is demonstrated by using inline orthogonal pumping scheme for midspan spectral inversion [17], [18]. In addition to orthogonal pumping scheme, there has been different approach is suggested and presented for wavelength conversion [19]–[22]. In these experiments, wavelength conversion by using cross-phase modulation (XPM) with nonlinear loop mirrors are demonstrated [19], [21]. However, multiple wavelength operation of wavelength converters based on XPM has not been discussed. In addition to having a polarization sensitivity, the additional crosstalk components due to different frequency pump lasers aggravates the challenge for wavelength-division-multiplexing (WDM) systems. Similar techniques, in addition to polarization diversity technique, are utilized for SOA and fiber distributed-feedback (DFB) laser-based wavelength converters [23]–[26].

Since the early experiments focus mainly on the enhancement of WDM system capacity by providing wavelength flexibility and wavelength reuse, the polarization insensitivity is limited to <7 nm and the crosstalk problem is overlooked [10], [27]. However, the increasing conversion efficiency leads to high crosstalk, which will be the second limitation of the wavelength converters when it used for conversion of high channel counts. In one of the previous experiments, the crosstalk values as high as -10 dB have been measured [10]. Since the number of channels used in these experiments was less than 7 nm, placement of inline filters has been proposed

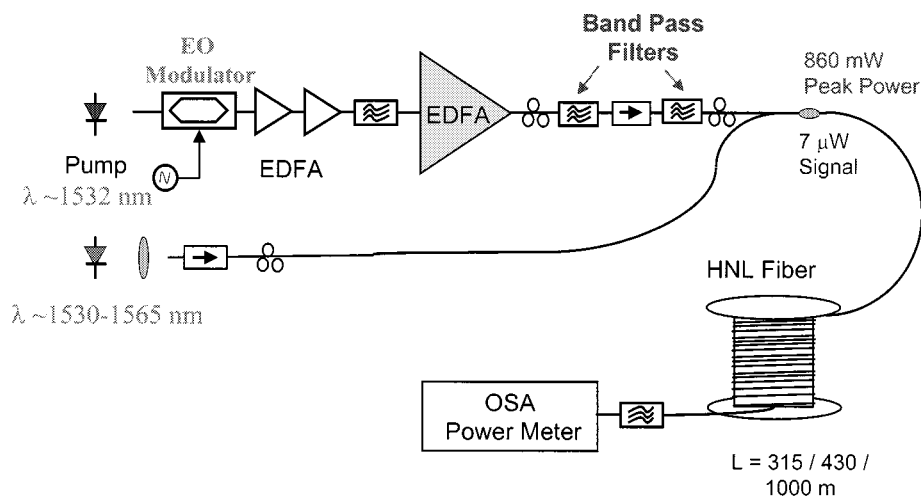


Fig. 2. Experimental setup of the straight fiber wavelength converter. Modulation instability in HNL-DS fibers converts the signal in the *C*-band to *S*-band by using 860-mW quasi-CW pump at 1532 nm. Gain profile, polarization sensitivity, and crosstalk are measured by using an optical spectrum analyzer (OSA) and a power meter.

to eliminate the crosstalk components [10], [28]. Although the filtering of crosstalk component will improve the system performance, it will not be effective or practical for dense WDM systems with channel spacing < 40 GHz and for elimination of inband crosstalk components. Yet, there has not been any kind of solution proposed to eliminate the crosstalk problem in dense WDM wavelength converters. The effect of large channels counts and channel spacing on crosstalk is considered only for WDM propagation and detection systems [29].

Thus, the polarization sensitivity and the crosstalk of parametric amplifiers remain a significant barrier for applications in WDM telecommunications systems. In the current experiment, we pay special attention to these two limitations. By identifying the reasons behind polarization sensitivity, crosstalk, and the coupling between these two problems, a loop configuration with optimized fiber length is proposed and implemented. System implications also discussed based on the low polarization sensitivity results.

III. STRAIGHT FIBER WAVELENGTH CONVERTER EXPERIMENT

The experimental setup used for crosstalk and polarization-sensitivity measurement in straight fiber is shown in Fig. 2. The pump laser is a quasi-CW source generated by a laser diode at 1532 nm with 20-mW output powers. Ideally, a CW source with high power and a phase modulator should be used. For following two practical challenges in the experiment, the quasi-CW source is used as a pump source: to suppress the Brillouin scattering and to reach the required peak power levels. To generate the quasi-CW, an electrooptic amplitude modulator is driven by RF signal at 4-MHz repetition rate with a 3% duty cycle. The peak pump power is set to be 860 mW after three stages of amplifiers with 1.5-mW, 7-mW, and 1-W saturated power levels and 4-, 7-, and 6-dB noise figure values. After the amplifiers, the accumulated amplified spontaneous emission (ASE) noise is filtered by bandpass filters with 2-nm bandwidth. Instabilities caused by back reflection are eliminated by a fiber isolator. The signal is generated by a free space coupled tunable CW laser

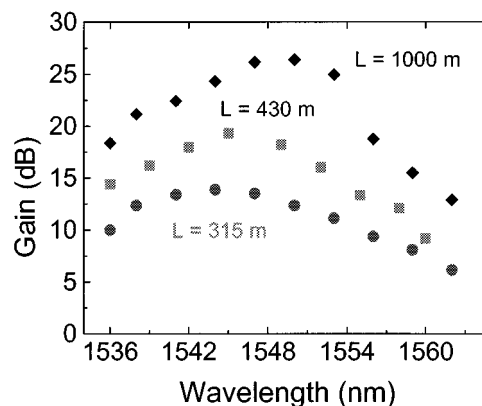


Fig. 3. The gain profile of the MI in the HNL-DS fiber. The gain profile of the MI is measured in 315 m, 430 m, and 1 km of HNL-DS fiber. The minimum conversion efficiency in 315-m fiber is calculated to be more than 4.7 dB.

diode. The signal is combined with the pump laser by a 5/95 fiber tap coupler after passing through an isolator. Two polarization controllers (PC) on the signal and the pump arm are used to adjust the relative polarizations to measure the worst-case crosstalk and polarization sensitivity values. The wavelength conversion is performed by modulation instability (MI) in the HNL-DS fiber with $\lambda_0 = 1530.34$ nm and dispersion slope of $\partial D/\partial \lambda = 0.026$ ps/nm².km. The pump and the signal powers in the HNL-DS fiber are 860 mW and 7 μ W, respectively. The measurements are performed after 315-m, 430-m, and 1-km HNL-DS fibers to show the length dependence of the crosstalk and polarization sensitivity. A power meter and an optical spectrum analyzer are used as diagnostic devices after filtering the converted signals.

Fig. 3 illustrates the measured gain curves by using 315 m, 430 m and 1 km HNL-DS fibers. The conversion bandwidth at 3-dB point is measured to be > 30 nm. This 30-nm conversion band shows that all the WDM channels within the *C*-band can be converted to the *S*-band. By using the minimum gain value of 6 dB obtained in 315-m HNL-DS fiber, the minimum conversion efficiency can be calculated as > 4.7 dB [27]. The gain profile is

determined by the MI used for wavelength conversion, and the gain uniformity is measured to be $\sim \pm 3.5$ dB in the 315-m fiber. Since the pump laser is located very close to the zero dispersion wavelength of the fiber, the fourth-order dispersion plays a significant role in the gain profile. Smoother decay at the edge of the gain bandwidth and larger conversion bandwidth is obtained because of the fourth-order dispersion and 1-dB/km loss in the fiber.

Channel crosstalk caused by nondegenerate four-wave mixing (FWM) is one of the limitations of MI based wavelength converters in system applications. From the beginning of the gain fiber, the amplification by MI effect and nondegenerate FWM develops simultaneously. Since the harmonic generated by the FWM is much smaller than the signal power at the initial stage, negligible crosstalk occurs. However, as the fiber length increase, the increasing harmonic power starts to interfere with nearby WDM channels and causes crosstalk between two channels. The crosstalk is calculated by the formula

$$X_{\text{talk}} = \frac{\sum P_{\text{harmonic}}}{P_{\text{signal}}} \quad (1)$$

where P_{harmonic} defines the total power of the unwanted signals generated by nondegenerate FWM. Typically, the strength of this harmonic is expected to be 25 dB below the signal power to minimize the interference and to achieve 10^{-10} bit error rate with 0.5-dB power penalty.

To measure the crosstalk between channels, the power of the harmonic generated by nondegenerate FWM and the signal power at the same wavelength are measured experimentally. Fig. 4(a) displays the calculated crosstalk at the end of 315-m HNL-DS fiber. Because of the efficient phase matching near the zero-dispersion wavelength, the strength of the crosstalk is measured to be -27 dB near the pump wavelength compared to the wavelengths near the edge of the conversion band. Since the phase mismatch increases at the wavelengths away from the pump, the strength of the crosstalk decreases. For channels >10 nm away from the pump wavelength, crosstalk values as low as -40 dB are measured. At wavelengths >20 nm away from the λ_0 of the fiber, the crosstalk values goes to lower than -40 dB. However, because of the instrument limitation, we consider -40 dB as the baseline in the experiment.

The strength of the harmonic, which causes crosstalk, is measured in 430-m and 1-km HNL fiber to show the effect of fiber length on crosstalk. Fig. 4(b) summarizes the strength of the harmonic after normalizing by $7\text{-}\mu\text{W}$ input signal power across the conversion band. For short fibers, the maximum crosstalk level is measured to be less than -27 dB, and it decreases exponentially at wavelengths away from the pump source. However, the pattern of the crosstalk changes drastically with further propagation in the fiber, as shown in Fig. 4(b). This change of crosstalk can be explained by the nonuniform increment in MI gain with further propagation. The effect of nonuniform gain profile on crosstalk pattern will be discussed in detail in Section VI. Because of high gain in the midband, the strength of the harmonic generated by channels with stronger gain is increased drastically as the gain accumulates with propagation. Therefore, the strengths of the harmonics at longer wavelength are expected to

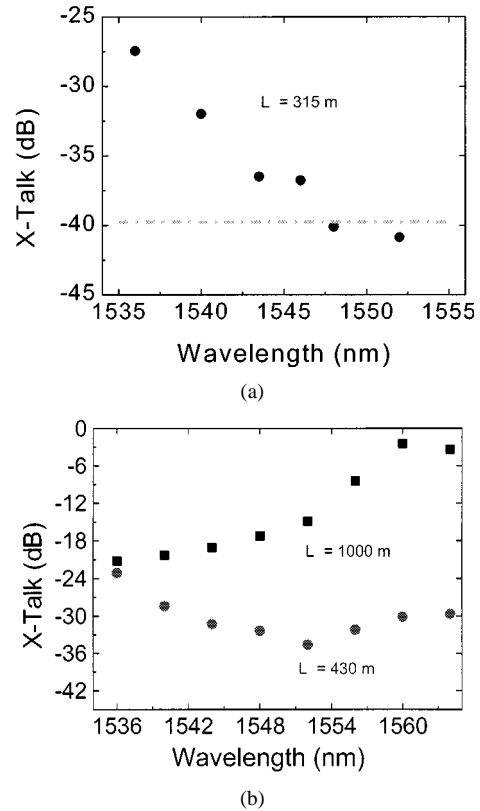


Fig. 4. Measured crosstalk patterns in short and long fibers. (a) In shorter fiber lengths, the nondegenerate FWM define the crosstalk pattern. Because of increasing phase mismatch decreasing crosstalk pattern is measured away from pump laser. (b) In longer fibers, the high gain and increasing signal power reverse the crosstalk pattern.

be stronger in longer fibers. Measurements in the 430-m HNL fiber show this increment at wavelengths >1550 nm. When the signals reach the end of 1-km fiber, the harmonics generated by the signals with high gain region will dominate the ones generated by weaker signals.

Experimental measurements confirm the expectations of decreasing crosstalk with -22 - and -5 -dB crosstalk at 1534 nm and at 1556 nm, respectively, as shown in Fig. 4(b). In other words, the strength of the generated crosstalk component reaches 5 dB below the input signal level in 430 m and 10 dB above the input signal power in 1 km at the same wavelengths. These results clearly demonstrate that for stable operation, the length of the gain medium should be optimized for low crosstalk at the expense of conversion efficiency. For the given experimental parameters, 315-m HNL-DS fiber can convert the whole C-band into S-band with <-27 -dB inband crosstalk. However, >2 -dB polarization sensitivity in the given setup is still a challenge to be addressed.

IV. POLARIZATION INSENSITIVE LOOPED FIBER BAND CONVERTER

A looped fiber wavelength converter configuration formed by a PBS with optimized fiber length is used for the polarization-insensitive wavelength conversion with low crosstalk. Fig. 5 shows the experimental setup used for low polarization sensitivity. Since the polarization sensitivity originates from the fact that relative polarization state of the signal and the pump

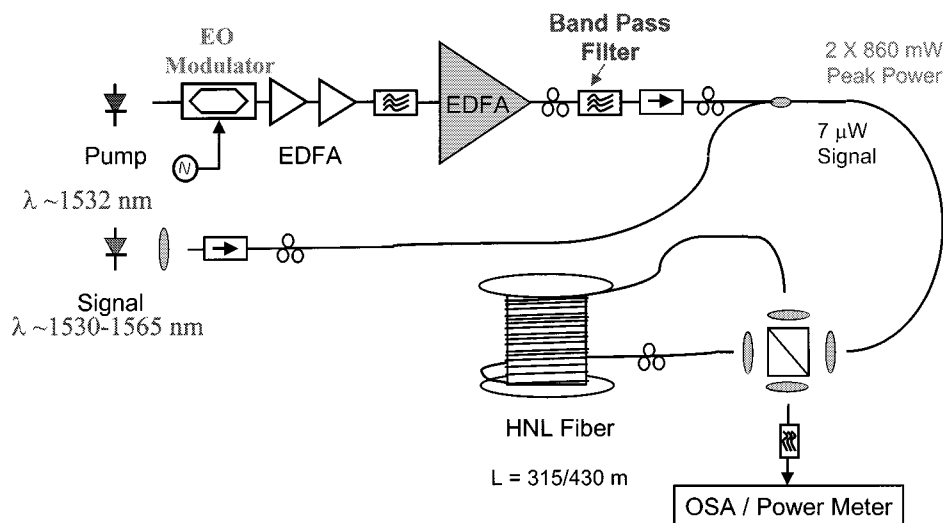


Fig. 5. Loop configuration for low polarization sensitivity wavelength converter. By using a PBS the relative polarization states of the pump and signal is fixed in the gain fiber. By strictly controlling the pump polarization equal amount of pump powers are sent in each direction of propagation.

change randomly and MI gain is different at orthogonal polarization states, an optical component should be used to preserve the polarization states in the fiber. Using the loop configuration with the PBS prevents random polarization changes between the pump and the signal and ensures that there will be the same amount of pump power propagating in each direction to obtain the same gain. Unlike conventional loop mirrors or Sagnac interferometers, the output port is defined by the polarization states of the converted signals instead of interference at the couplers. In the experiment, to satisfy the requirement of equal pump power in each arm, the power levels of the pumps are first equally distributed and fixed to 860 mW in each polarization component by adjusting the polarization controller (PC) in the pump arm. The direction of propagation in the configuration is set by the ports of the PBS, and each polarization state propagates through the same fiber in opposite directions. To maintain the relative polarization states of the pump and the signal in the converter, the incoming signal is split in two by the same PBS. After the wavelength conversion process, the converted signals are coupled out through the same PBS for diagnostics. The PC in the loop is inserted to make sure that all the signal and pump beams exit through the output port of the PBS. To measure the polarization sensitivity of the device, the PC in signal arm is adjusted to measure the maximum and the minimum gain values.

Fig. 6 illustrates the polarization sensitivity measured in 315- and 430-m fibers for both the straight fiber and the looped fiber experiments across the whole conversion bandwidth. The polarization sensitivity of the wavelength converter is calculated after measuring the maximum and the minimum gain with respect to signal polarization. The formula used for calculation of polarization sensitivity is

$$P_{sen} \text{ (dB)} = G_{max} \text{ (dB)} - G_{min} \text{ (dB)} \quad (2)$$

where G_{max} and G_{min} represent the maximum and the minimum gain measured for different polarization states of the incoming signal. The maximum polarization sensitivity is measured to be 0.65 dB in 315 m, as shown Fig. 6(a). Compared to

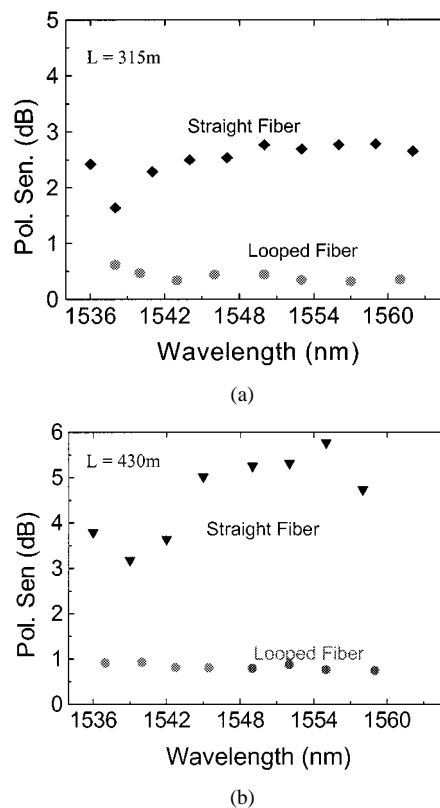


Fig. 6. Comparative polarization sensitivity results. (a) Maximum polarization sensitivity is measured to be <0.65 dB in 315 m, which is 2 dB better than the straight fiber results. (b) In 430 m, the maximum polarization sensitivity is measured to be less than 0.9 dB, which is 4.5 dB better than the straight fiber wavelength converter with the same 430-m fiber lengths.

the straight fiber, >2-dB improvement in polarization sensitivity is measured across the most of the conversion bandwidth. When the fiber length is increased to 430 m, the maximum polarization sensitivity is measured to be 0.9 dB in the looped fiber, as shown in Fig. 6(b). Compare to the straight fiber experiment with the same fiber length of 430 m, as high as 4.5-dB improvement in polarization sensitivity is measured. The only difficulty arises due to the temperature dependent birefringence of the gain fiber

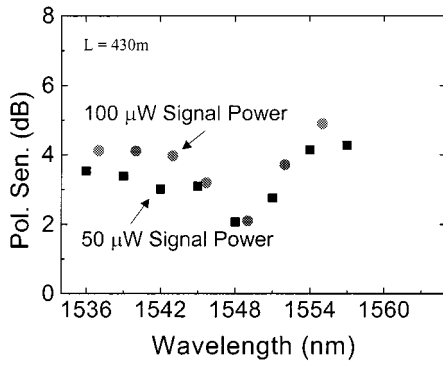


Fig. 7. Effect of signal power on polarization sensitivity. Because of coupling between the polarization sensitivity and crosstalk, the pattern of polarization sensitivity changes in longer fiber lengths. The figure shows the polarization sensitivity in 430-m HNL-DS fiber for 50- and 100- μ W signal powers.

or mechanical vibrations, which causes amplitude fluctuations at the output port because of polarization changes in the gain fiber. As long as the gain fiber is fixed and temperature stabilized, <0.6-dB low polarization sensitivity is maintained. To eliminate the thermal or other effects on the gain fiber, a polarization-maintaining fiber can be used within the loop as an alternative approach.

The reason behind the ~ 0.25 dB change in polarization sensitivity by increasing the fiber length from 315 to 430 m is also investigated experimentally. In this part of the experiment, it is shown that the gain and signal power level are critical parameters for polarization-insensitive wavelength conversion. In the results of Fig. 6, it is measured that for 7- μ W signal power level the polarization sensitivity is degraded by 0.25 dB as the fiber length is changed from 315 to 430 m. This change indicates that there is a coupling between the amount of energy transferred to the harmonic, i.e., crosstalk and the polarization sensitivity.

To check the power dependency of the polarization sensitivity, the polarization sensitivity at the end of 430-m looped fiber is measured for 50- and 100- μ W signal power levels. The results of the power dependent polarization sensitivity measurements are shown in Fig. 7. The results show that as the signal power is amplified, the increasing crosstalk causes degradation in polarization sensitivity as large as 4 dB. Therefore, to generate environmentally stable WDM signals by converting the existing sources in the C-band, the fiber length and signal power level should also be optimized. Based on the experimental results, fiber lengths ~ 315 m with signal power levels as low as 7 μ W can be used for stable operation with the given experimental parameters.

V. THEORETICAL RESULTS

The experimental results for polarization sensitivity and crosstalk are also verified with simulations. In the simulations, the nonlinear Schrödinger equation (NLSE) is used to calculate the wavelength conversion, taking into account all of the interactions between different frequency components instead of dealing with each frequency component separately. In particular, the accumulated MI gain, crosstalk, polarization sensitivity, and the coupling between the crosstalk and the polarization sensitivity across the gain bandwidth are estimated

by solving the NLSE equation [17]. Two coupled NLSE equations used for wavelength conversion are given by

$$\begin{aligned} \frac{\partial A_x}{\partial z} + \frac{i}{2} \beta_2 \frac{\partial^2 A_x}{\partial t^2} - \frac{i}{6} \beta_3 \frac{\partial^3 A_x}{\partial t^3} + \frac{i}{24} \beta_4 \frac{\partial^4 A_x}{\partial t^4} \\ = i\gamma \left\{ |A_x|^2 + \frac{2}{3} |A_y|^2 \right\} A_x + i \frac{\gamma}{3} A_x^* A_y^2 e^{i2(2\pi\Delta n/\lambda)z} \end{aligned} \quad (3a)$$

$$\begin{aligned} \frac{\partial A_y}{\partial z} + \frac{i}{2} \beta_2 \frac{\partial^2 A_y}{\partial t^2} - \frac{i}{6} \beta_3 \frac{\partial^3 A_y}{\partial t^3} + \frac{i}{24} \beta_4 \frac{\partial^4 A_y}{\partial t^4} \\ = i\gamma \left\{ |A_y|^2 + \frac{2}{3} |A_x|^2 \right\} A_y + i \frac{\gamma}{3} A_y^* A_x^2 e^{-i2(2\pi\Delta n/\lambda)z}. \end{aligned} \quad (3b)$$

The terms β_2 and β_4 represent the second-order and the fourth-order dispersion parameters, which mainly determine the phase-matching condition and the amount of gain for MI. Although the third-order dispersion β_3 does not contribute to the MI gain, it significantly changes the efficiency of the harmonic generation and the crosstalk. The nonlinear parameters on the right side are the self-phase modulation, which determines the wavelength conversion among the signal with the same polarization and power dependent phase mismatch, and the XPM terms. The coupling between the orthogonal axis components is defined by the XPM term. The final terms on the right side shows the effect of the background birefringence. The parameter $2\pi\Delta n/\lambda$ is the phase mismatch caused by the background birefringence Δn , where Δn is measured to be $\sim 5 \times 10^{-6}$ in the fiber used in the experiment. Since the beat length, ~ 30 cm, caused by this birefringence is much smaller than the total fiber length and the length of the random axis change the effect of Δn averages to zero. To simulate the effect of random axis changes, we used 20 segments in the simulations, where the birefringence axis is changed randomly between the segments. The other parameters used in the simulations are $\beta_2 = 0.053$ ps²/km, $\beta_3 = 0.041$ ps³/km, $\beta_4 = 7$ ps⁴/km, and $\gamma = 9.9$ W⁻¹ · km⁻¹. The fiber loss is 0.8 dB/km. Additionally, the pump is defined as a perfect CW source. The simulation bandwidth starts from 1485 to 1585 nm. 0.5-GHz frequency resolution, which corresponds 2-ns time window, with 32 768 numbers of points is used in the simulations. To measure the polarization sensitivity, the signal polarization states are changed relative to pump. However, signals are aligned parallel to calculate the worst case of crosstalk. The split step Fourier method is used to solve the NLSE [30].

The calculation of the crosstalk between the channels is the first part of the simulations. The signal level is chosen to be 7 μ W and fiber lengths are set to be 315 m, 430 m, and 1 km in the simulations to match the experimental parameters. As a pump power, we use the same power level (860 mW) used in the experiment. Fig. 8(a) shows the estimated crosstalk at the end of 315-m HNL-DS fiber. Less than 3-dB differences in crosstalk values are calculated at wavelengths near zero dispersion wavelength (λ_0) compare to the experimental measurements. This difference can be explained by high level of amplified spontaneous emission (ASE) noise near the pump wavelength. When we move away from the λ_0 of the fiber, the difference between calculations and the measurements drops to <0.5 dB by the effect of filters used to eliminate ASE. For the wavelengths beyond 1550 nm, the instrument sensitivity sets the boundary of

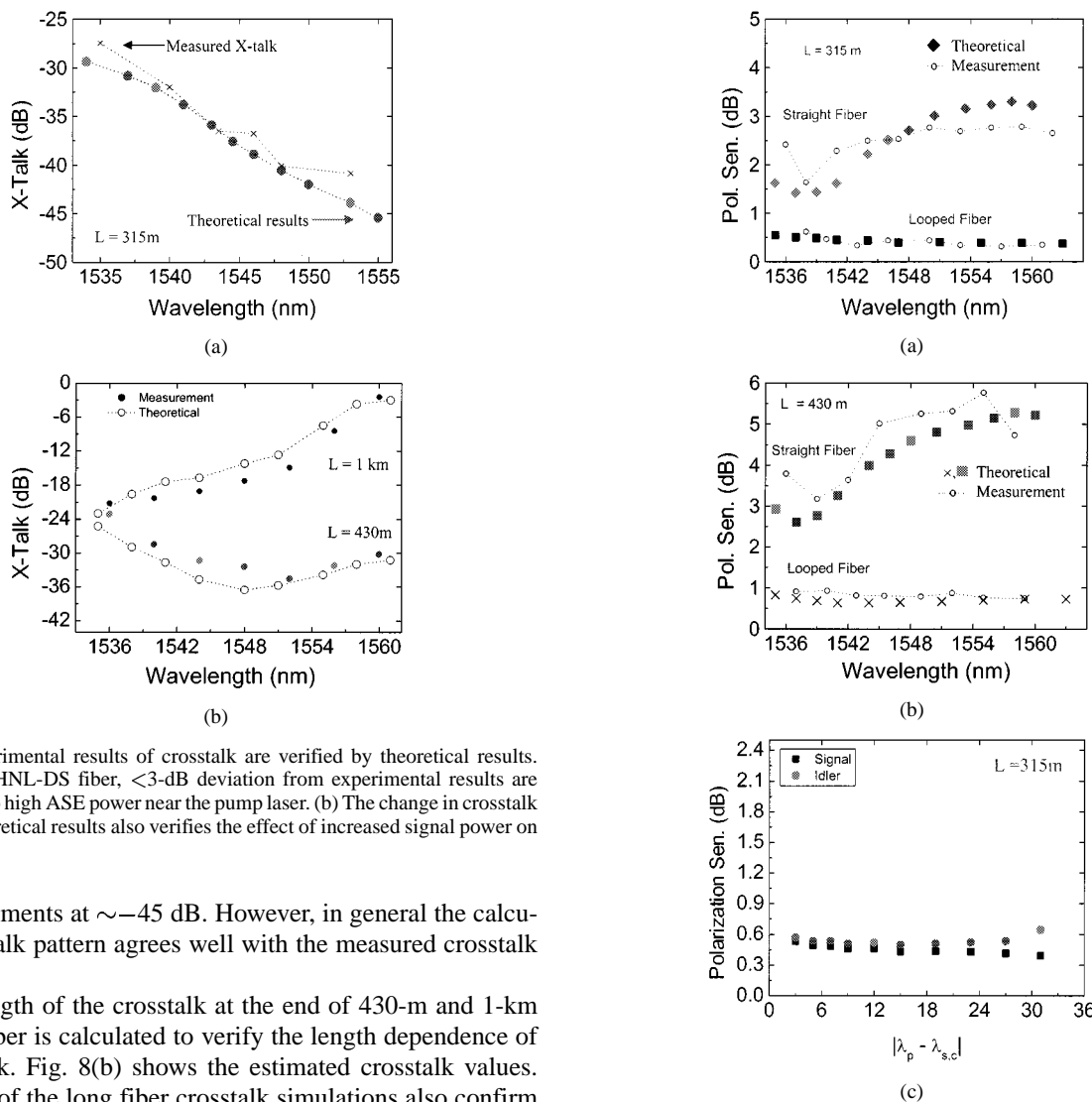


Fig. 8. Experimental results of crosstalk are verified by theoretical results. (a) In 315-m HNL-DS fiber, <3-dB deviation from experimental results are obtained due to high ASE power near the pump laser. (b) The change in crosstalk pattern in theoretical results also verifies the effect of increased signal power on crosstalk.

the measurements at ~ -45 dB. However, in general the calculated crosstalk pattern agrees well with the measured crosstalk pattern.

The strength of the crosstalk at the end of 430-m and 1-km HNL-DS fiber is calculated to verify the length dependence of the crosstalk. Fig. 8(b) shows the estimated crosstalk values. The results of the long fiber crosstalk simulations also confirm the experimental results with less than 2-dB difference at wavelengths near the pump laser. These simulation results show that there are two mechanisms that define the strength of the crosstalk. The first mechanism is the FWM conversion efficiency, which is set by the phase mismatch. Theoretically, the FWM conversion efficiency is higher near the zero dispersion wavelength. The second mechanism is the strength of the signal. Since the strength of the harmonic is proportional to signal power, nonuniform gain patterns alter the crosstalk pattern. Therefore, the crosstalk pattern in short fiber lengths is mainly set by the FWM conversion efficiency. On the other hand, increasing fiber length creates stronger signals away from λ_0 of the fiber, which creates stronger harmonics toward the edge of the conversion bandwidth. Based on these simulations and the experimental results, we conclude that shorter fiber lengths are required for band conversion with < -25 -dB inband crosstalk, which means a compromise in conversion efficiency for WDM applications.

The theoretical results also verify the improvement as high as 2.5 dB in the polarization sensitivity by using the loop configuration. Similar to the experimental procedure, the polarization sensitivity in the straight fiber and the looped fiber are calculated, and the results are compared. Based on the modeling of the straight fiber experimental setup with 315- and 430-m

Fig. 9. The polarization sensitivity results are verified by simulations. (A) In 315-m HNL-DS fibers, low polarization sensitivity of < 0.5 dB is estimated for looped case. > 2.5 -dB improvements in polarization sensitivity are estimated compare to straight fiber. (b) Polarization sensitivity of < 0.8 dB is calculated in 430-m fibers. (c) Theoretical results show that similar polarization sensitivity is expected at the converted band as the conversion efficiency exceeds 3 dB. For 4.7-dB conversion efficiency, the difference in polarization sensitivities is < 0.1 dB.

HNL-DS fibers, the polarization sensitivity of ~ 3 and 5.5 dB is calculated, respectively. In 315-m HNL fiber, using the loop configuration reduces theoretically the polarization sensitivity to 0.5 dB. The experimental results match the theoretical results with < 0.5 -dB deviation in straight fiber configuration, as shown in Fig. 9(a). The deviation happens mainly near the pump wavelength, where the ASE is strongest. The deviation near the gain peak can be explained by the 2-dB difference in calculated and measured gain values. For the looped fiber case, the deviation is < 0.1 dB, and the measurements follow the theoretical results closely. Fig. 9(b) illustrates the polarization sensitivity results for 430-m HNL fiber. Similar to 315-m results, < 0.2 deviation in theoretical and experimental results are obtained. To show the effect of larger signal power, the polarization sensitivity is calculated with 50- and 500- μ W signal power levels. The results show that the increased crosstalk alters the polarization sensi-

tivity as much as 4 dB in 400-m long fibers for 50- μ W channel power. These results also show that the increasing crosstalk couples the polarization sensitivity and the crosstalk. Therefore, along with the length optimization, signal power levels should be adjusted for stable operation.

To show that the same trend of the polarization sensitivity is followed in idler side, we simulate the polarization sensitivity of the converted band [Fig. 9(c)]. The results show that the similar polarization sensitivity, ~ 0.6 dB for the worst case, will be obtained in the converted band. The deviation at the longer wavelengths arise from the fact that the conversion efficiency at wavelength separation >20 nm decreases and it leads to more polarization sensitivity. This similarity in polarization sensitivity is expected because of the fact that the MI is a three photons processes, i.e., the same amount of photon will be generated in the signal band and in the converted band. Therefore, any fluctuation in the amount of photon generation in signal band will be reflected into the converted band and the similar polarization sensitivity will be obtained. More specifically, the amount of photon generated in both signal and idler band can be expressed by the conversion efficiency equation

$$\eta = (\gamma P_0 L)^2 \frac{\sinh^2(g_0 L)}{(g_0 L)^2}. \quad (4)$$

Similarly, the gain in the signal band is defined by

$$G = (\gamma P_0 L)^2 \frac{\sinh^2(g_0 L)}{(g_0 L)^2} + 1 \quad (5)$$

where $g_0 = \Delta k + 2\gamma P = \sqrt{-\Delta\beta((\Delta\beta/4) + \gamma P_0)}$, and $\Delta k = k_s + k_c - 2k_p$. The $\Delta\beta$ in equation represent the phase mismatch caused by group velocity dispersion. The difference in polarization sensitivity in idler and signal band will be created by the term “+1” on the rightmost side of the gain equation [(5)]. As long as conversion efficiency is >3 -dB polarization sensitivities will be similar. The difference of ~ 0.1 dB reflects the effect of the term “1” in the equation for the conversion efficiency of 4.7 dB.

VI. SYSTEM PERFORMANCE OF CONVERTED SIGNALS AND EFFECT OF PUMP NOISE

The usefulness of the wavelength converter in a real system is the main question that should be answered before comparing the current experimental results to the results of the previous experiments. To answer this question, a 32-channel WDM transmission system is modeled with 1-mW/Ch power level at the beginning of the transmission fiber and 100-GHz channel spacing in the *C*-band and in the *S*-band. In the simulations, the polarization states of the signals are changed relative to polarization state of the pump laser to estimate the system performance. However, the polarization states of the signals kept the same to estimate the worst case of crosstalk. To compare the performance of the WDM signals generated by laser diodes and the WDM signals generated by the polarization-insensitive band converter, the optical signal-to-noise ratio (OSNR) degradation is calculated at the end of the transmission line. The noise calculation is performed within ± 50 -GHz filter bandwidth. A 5-dB noise figure of the amplifier in each span is also included. The length of the transmission line is set to be 800 km with standard communication fiber and amplifier span of 80 km.

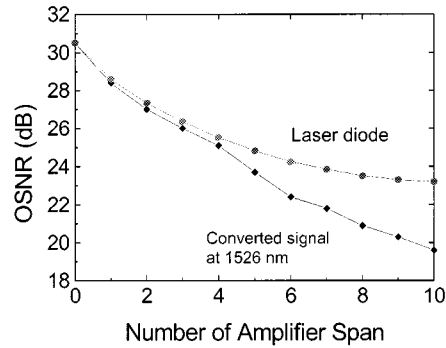


Fig. 10. OSNR degradation of laser diodes and the converted signals. Theoretically, 32-channel converted signals without gain equalization and noise filtering propagated through 800-km SMF with 80-km amplifier span. Compare to laser diodes, 3.6 dB higher OSNR degradation is estimated at the end of ten amplifier span.

For the transmission of WDM channels generated by laser diodes, OSNR degradation is calculated by assuming no nonlinear interactions occur during the propagation. To calculate the OSNR degradation, the accumulated ASE power in each amplifier is calculated by the equation

$$P_{\text{ASE}} = (G - 1).NF.h.\nu.B_o \quad (6)$$

where G is the amplifier gain, NF is the noise figure of the amplifier, and B_o is the optical bandwidth of the filter [31]. The parameter ν defines the operation frequency and h is the Planck's constant. Since cascaded amplification is used in the simulation, the final value of the OSNR at the end should be calculated. If we assume identical amplifiers with uniform insertion loss in the fiber, then the OSNR value at the end of N amplifier span, SNR_N , can be calculated as

$$\text{SNR}_N = \frac{\text{SNR}_i.P_{in}}{P_{in} + (1 + \text{SNR}_i)(G - 1).N.NF.h.\nu.B_o} \quad (7)$$

where SNR_i is the OSNR value before the propagation system. The total loss in each section is assumed to be equal to the gain of the amplifier.

In the first step, the converted signals without gain equalization are propagated through 800-km transmission line. The power level at 1526 nm is set to be 1 mW without changing the gain profile. The initial OSNR of the converted signal at 1526 nm is calculated to be ~ 30.4 dB after wavelength converter. For a fair comparison, the OSNR of the laser diode is also set to be 30.4 dB. Fig. 10 illustrates the OSNR degradation of both the converted signal and the laser diode. The final OSNR value is calculated due to the polarization sensitivity and the crosstalk generated during the band conversion. Ignoring the nonlinear effects during the transmission, an ITU grid laser diode results in an OSNR value of 23.2 dB at the end of ten-span transmission distance. However, because of the nonuniform signal powers, ~ 33 -dB inband crosstalk and 0.45-dB polarization sensitivity [Fig. 9(c)], where polarization sensitivity introduces amplitude modulation on the signal, the OSNR value of the converted signal is estimated to be ~ 3.6 dB lower than the laser diode, as shown in Fig. 10. In other words, for the receiver sensitivity set to be 24-dB OSNR value, the difference in maximum propagation length is estimated to be 240 km, i.e., three amplifiers span.

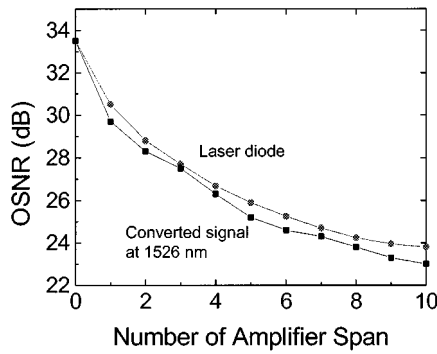


Fig. 11. By using gain equalization after the wavelength conversion and setting the spacing between the first channel and the pump as three times the channel spacing, the OSNR degradation is reduced to 0.7 dB at the end of ten amplifier spans.

The system performance of the converted signals can be further improved by adjusting the design parameters. The first change in the simulations is introducing gain equalization. In the second part of the simulations, the intensities of the WDM channels are set to be 1 mW. In addition, to reduce inband crosstalk, the spacing between the first WDM channel and the pump is adjusted. By choosing the spacing as odd multiples of the channel spacing, the inband crosstalk can be minimized. Since most of the crosstalk components will be accumulated in the middle of two channels, further reduction in crosstalk values can be achieved by introducing periodic grating filters or solid etalons. In the simulations, the spacing between the first channel and the pump is set to be three channels spacing, i.e., 300 GHz. Additionally, by using a solid etalon with finesse of ten, an additional ~ 6 -dB reduction in out-of-band crosstalk is introduced. Fig. 11 shows the OSNR degradation in the *S*-band and in the *C*-band along the transmission fiber for a channel located at 1526 nm and the image of the channel in the *S*-band. Ignoring the nonlinear effects during the propagation, OSNR drops by ~ 10 dB from 33.5-dB initial OSNR value at the end of ten amplifier span. Compare to commercial lasers, having an additional 0.7-dB OSNR degradation shows less than one span penalty for the receiver sensitivity of 24 dB.

The effect of the pump noise on converted signals will be another determining factor for the system performance of the band converter. Previously, the noise figure of parametric amplifiers has been calculated for different fiber types and optimum fiber length has been proposed for dispersion shifted fibers [32], [33]. To enumerate the performance degradation, relative intensity noise (RIN) degradation along the conversion band during the wavelength conversion process is calculated analytically. In the calculations, we focus on the transfer of the pump amplitude noise to the converted signal. Since the experiments were conducted in nonpump depletion regime, the calculations ignore the pump depletion. Also, because the primary focus is on the amount of RIN degradation on converted signals due to pump RIN, the noise coming from the signals are ignored. Starting with the three wave interactions, the conversion efficiency at the end of a fiber length L in the nonpump depletion regime can be formulated as

$$\eta = (\gamma P_0 L)^2 \frac{\sinh^2(g_0 L)}{(g_0 L)^2} \quad (8)$$

where P_0 is the average pump power and g_0 is the modified phase mismatch factor, which is given by

$$g_0 = \Delta k + 2\gamma P = \sqrt{-\Delta\beta \left(\frac{\Delta\beta}{4} + \gamma P_0 \right)}, \quad \Delta k = k_s + k_c - 2k_p. \quad (9)$$

To calculate the RIN degradation, the pump laser is modulated by a single tone noise source at frequency ω

$$E_p = E_p(1 + m \cos(\omega t)) \quad (10)$$

where m defines the modulation index of the pump laser. The RIN of the pump laser according to this definition can be formulated as [34]

$$\text{RIN}_p = 10 * \log \left(\frac{P_{\text{noise}}}{P_{\text{signal}}} \right) \cong 10 * \log(2m^2). \quad (11)$$

After adding the small perturbation caused by the modulation to the gain formula in nonpump depleted regime, the noise power at frequency ω can be calculated. The estimated RIN value of the signal is given by

$$\text{RIN}_s = \frac{1}{4} \left(4 + 2 \frac{\Delta\beta \gamma P_0}{g_0^2} + \frac{\gamma P_0 \Theta \sinh(2g_0 L)}{\sinh^2(g_0 L)} \right)^2 * \text{RIN}_p. \quad (12)$$

The first term in the numerator defines the RIN degradation due to power dependence of the phase mismatch term, and the second term defines the RIN degradation due to power dependence of the parametric gain. An additional weak RIN degradation occurs due to amplitude variation by noise, which is included in the last term in the numerator. The phase mismatch is included in parameter Θ , and it is formulated as

$$\Theta = L \sqrt{\frac{-\Delta\beta}{\frac{\Delta\beta}{4} + \gamma P_0}}. \quad (13)$$

Fig. 12 shows the estimated RIN degradation in 315-m, 430-m, and 1-km HNL-DS fiber. The analytical calculations show that RIN of the pump laser is also a limiting factor for system applications. The derivation indicates that the RIN of the pump laser completely transfers to the converted signals, with an additional RIN degradation factor caused by pump square dependence of the gain and power dependent phase mismatch factor. It is also shown that the fiber length of the wavelength converter affects the RIN degradation. For the optimized fiber length of 315 m, the maximum RIN degradation is estimated to be < 12 dB/Hz. As the wavelength separation increases, the RIN degradation increases because of increasing gain values. For fiber lengths of 1 km, the additional RIN degradation reaches as high as 20 dB/Hz. When the wavelength separation reaches the $g_0 = 0$ point, the additional RIN degradation reduces to 6 dB/Hz because of the perfect phase match and parabolic gain. For wavelengths very close to pump wavelength, an additional length independent ~ 6 dB/Hz additional RIN degradation is estimated. The 6-dB/Hz RIN degradation near pump wavelength comes from the fact that the gain is parabolic in that region. These results indicate that in addition to polarization sensitivity and crosstalk of the band converter, the RIN of the pump laser will limit the system performance. If the requirement for converted signal is RIN values < -140 dB/Hz, then a pump laser with < -155 dB/Hz must be used.

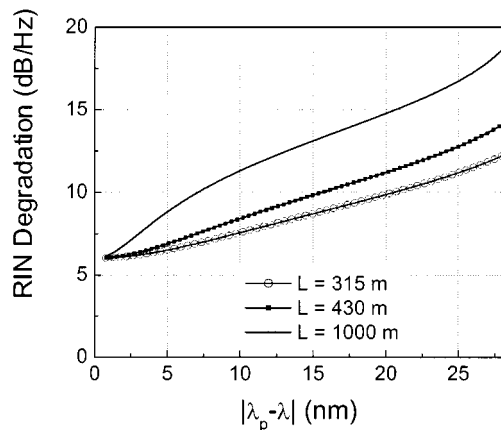


Fig. 12. RIN degradation due to pump noise. The RIN degradation due to amplitude fluctuations on the pump laser is estimated analytically. The results show <12 -dB/Hz RIN degradation in 315-m optimized fiber length and degradation get worse for longer fiber lengths. As high as 20-dB/Hz RIN degradation occurs at the end of 1 km in nonpump depleted regime.

VII. DISCUSSION

The focus in our experiments has been on the system performance of the wavelength converter rather than the conversion efficiency. The experimental results show that broad-band, >30 nm, wavelength conversion with low polarization sensitivity, <0.65 dB, low crosstalk, <-27 dB, high conversion efficiency, >4.7 dB, can be achieved simultaneously. Although the wavelength conversion schemes demonstrated before result in low polarization sensitivity (<1.2 dB), the low polarization sensitivity is confined within <7 nm bandwidth. In the current experiments, the polarization sensitivity is improved by >0.5 dB over >30 -nm conversion bandwidth by using the loop configuration with HNL-DS fiber. Moreover, the high conversion efficiency and low crosstalk requirements are satisfied simultaneously. Compared to the low polarization sensitivity results, the conversion efficiency is improved by >20 dB while maintaining the crosstalk <-27 dB, which corresponds ~ 15 -dB improvement across the whole >30 conversion bandwidth, by optimizing the fiber length and signal power according to system requirements.

Although higher conversion efficiency, >30 dB, is used as a figure-of-merit in some experiments, the experimental results show that the higher crosstalk accompanied by higher conversion efficiency will limit the applicability of the wavelength converter. Based on the experimental and theoretical results, it is reasonable to conclude that new communication bands sources can be made by using the existing sources in the C -band with an optimized wavelength converter. The estimation of <0.8 -dB OSNR degradation in 800-km standard communication fiber indicates that stable WDM sources can be generated in the S -band or L -band by using the wavelength converter with optimized loop configuration. However, since the intensity noise of the pump laser will be transferred to converted signals, high power lasers with <-155 -dB/Hz RIN values should be used as a pump source to overcome the pump noise limitations.

VIII. SUMMARY

In the modulation instability based wavelength converter experiment, conversion of readily available sources in the C -band

into the S -band is demonstrated by using a tunable signal source with tuning range >40 nm. More than 30-nm conversion bandwidth with greater than 4.7-dB conversion efficiency is measured in 315 m of high-nonlinearity dispersion-shifted fiber by using 860-mW pump power at ~ 1532 nm. The polarization sensitivity and the channel crosstalk are determined to be the main obstacles for system applications, where the polarization sensitivity results from the random evolution of the incoming signal polarization. A loop configuration with PBS and optimized fiber length is implemented to solve the both problems simultaneously. By using the PBS, the relative polarizations of the pump and the signal are fixed in the gain fiber. Additionally, using the same fiber for both polarization states eliminates the gain difference due to different fiber lengths. With this technique, the polarization sensitivity is reduced to less than 0.65 dB in 315-m-high nonlinearity fiber. Compare to the conventional, fiber-based wavelength conversion scheme, about 2-dB improvement in polarization sensitivity is measured. In 430-m fiber, the maximum polarization sensitivity is measured to be <0.9 dB with 4.5-dB improvement compared to the conventional wavelength conversion scheme.

In addition, the maximum channel crosstalk is measured to be <-27 dB in 315-m fiber. In a detailed study of the crosstalk, the pattern of the crosstalk in short fiber lengths and long fiber lengths are measured. In short fiber lengths, the exponential decay in harmonic power shows that nondegenerate FWM determines the amount of the crosstalk. As the fiber length increases, the high signal power reverses the crosstalk pattern. Harmonic power 10 dB higher than the input signal power is measured at 1556 nm in 1 km of high nonlinearity dispersion-shifted fiber. The results also show that increasing the fiber length and channel power will couple the polarization sensitivity and the crosstalk, thereby degrading the polarization sensitivity as much as 4 dB in 430-m fibers.

The simulation results are in good agreement with the experimental measurements as well. The results indicate that by using length optimized loop configuration, the whole C -band can be converted to S -band, even L -band, with appropriate selection of the fiber and the pump. Using the loop configuration with optimized length will generate multiple wavelength sources with <0.65 -dB polarization sensitivity, low crosstalk, and high conversion efficiency. The system performance modeling of the band converter shows that the converted 32-channel WDM signals give as good performance as laser diodes. The OSNR degradation compared to laser diodes is calculated to be 0.7 dB after 800-km SMF fiber with 80-km amplifier span. However, due to pump fluctuations coupling and becoming accentuated in the nonlinear wavelength conversion process, the high powered pump must have a RIN <-155 dB/Hz.

REFERENCES

- [1] K. Inoue and H. Toba, "Wavelength conversion experiment using fiber four-wave mixing," *IEEE Photon. Technol. Lett.*, vol. 4, pp. 69–72, Jan. 1992.
- [2] M. E. Marhic, N. Kagi, T. K. Chiang, and L. G. Kazovsky, "Broadband fiber optical parametric amplifiers," *Opt. Lett.*, vol. 21, pp. 573–575, Aug. 1996.
- [3] M. Westlund, J. Hansryd, P. A. Andrekson, and S. N. Knudsen, "Transparent wavelength conversion in fiber with 24 nm pump tuning range," *Electron. Lett.*, vol. 38, pp. 85–86, Feb. 2002.

- [4] M. E. Marhic, Y. Park, F. S. Yang, and L. G. Kazovsky, "Broadband fiber optical parametric amplifiers and wavelength converters with low ripple Chebyshev gain spectra," *Opt. Lett.*, vol. 21, no. 17, pp. 1354–1356, 1996.
- [5] O. Aso, Y. Tashiro, M. Tadakuma, and S. Namiki, "Effect of modulational instability on broadband wavelength conversion using four-wave mixing in optical fiber," in *Optical Fiber Communication Conf.*, vol. 3, Baltimore, 2000, Paper ThL6, pp. 187–189.
- [6] O. Aso, S. I. Arai, T. Yagi, M. Tadakuma, Y. Suzuki, and S. Namiki, "Broadband wavelength conversion using a short high nonlinearity non polarization maintaining fiber," in *Proc. Eur. Conf. Optical Communication, ECOC*, vol. 2, 1999, pp. 226–227.
- [7] M.-C. Ho, M. E. Marhic, Y. Akasaka, and L. G. Kazovsky, "Fiber optical parametric amplifier and wavelength converter with 208 nm gain bandwidth," in *CLEO'2000 Tech. Dig.*, 2000, Paper CThC6, pp. 401–402.
- [8] M.-C. Ho, K. Uesaka, M. Marhic, Y. Akasaka, and L. Kazovsky, "200-nm bandwidth fiber optical amplifier combining parametric and Raman gain," *J. Lightwave Technol.*, vol. 19, pp. 977–981, July 2001.
- [9] M. Marhic, F. S. Yang, M.-C. Ho, and L. G. Kazovsky, "High-nonlinearity fiber optical parametric amplifier with periodic dispersion compensation," *J. Lightwave Technol.*, vol. 17, pp. 210–215, Feb. 1999.
- [10] J. P. R. Lacey, S. J. Madden, M. A. Summerfield, R. S. Tucker, and A. I. Faris, "Four channel WDM optical phase conjugator using four-wave mixing in a single semiconductor optical amplifier," *Electron. Lett.*, vol. 31, no. 9, pp. 743–744, 1995.
- [11] K. Inoue, "Polarization effect on four-wave mixing efficiency in a single-mode fiber," *IEEE J. Quantum Electron.*, vol. 28, pp. 883–894, Feb. 1992.
- [12] R. M. Jopson and R. E. Tench, "Polarization-independent phase conjugation of lightwave signals," *Electron. Lett.*, vol. 29, no. 25, pp. 2216–2217, 1993.
- [13] P. O. Hedekvist, M. Karlsson, and P. A. Andrekson, "Polarization dependence and efficiency in a fiber four-wave mixing phase conjugator with orthogonal pump waves," *IEEE Photon. Technol. Lett.*, vol. 8, pp. 776–778, June 1996.
- [14] K. Inoue, "Polarization independent wavelength conversion using fiber four-wave mixing with two orthogonal pump lights of different frequencies," *J. Lightwave Technol.*, vol. 12, pp. 1916–1920, Nov. 1994.
- [15] T. Hasegawa, K. Inoue, and K. Oda, "Polarization independent frequency conversion by four-wave mixing with a polarization diversity technique," *IEEE Photon. Technol. Lett.*, vol. 5, pp. 947–949, Aug. 1993.
- [16] J. P. R. Lacey, S. J. Madden, and M. A. Summerfield, "Four channel polarization insensitive optically transparent wavelength converter," *IEEE Photon. Technol. Lett.*, vol. 9, pp. 1355–1357, Oct. 1997.
- [17] S. Y. Set, R. Girardi, E. Riccardi, B. E. Olsson, M. Puleo, M. Ibsen, R. I. Laming, P. A. Andrekson, F. Cisternino, and H. Geiger, "Field transmission over 40 Gb/s using midspan spectral inversion," in *Proc. 24th Eur. Conf. Optical Communications, ECOC*, Madrid, Spain, 1998, p. 3.
- [18] —, "40 Gb/s field transmission over standard fiber using midspan spectral inversion for dispersion compensation," *Electron. Lett.*, vol. 35, pp. 581–582, July 1999.
- [19] B.-E. Olsson, P. Ohlen, L. Rau, and D. Blumenthal, "A simple and robust wavelength converter using fiber cross phase modulation and optical filtering," *IEEE Photon. Technol. Lett.*, vol. 12, pp. 846–848, July 2000.
- [20] B. E. Olsson and P. A. Andrekson, "Polarization independent all-optical AND-gate using randomly birefringent fiber in a nonlinear optical loop mirror," in *Proc. Optical Fiber Communication Conf., OFC*, vol. 2, 1998, pp. 375–376.
- [21] J. Yu, X. Zheng, C. Peucheret, A. T. Clausen, H. N. Poulsen, and P. Jeppesen, "40-Gb/s all-optical wavelength conversion based on a nonlinear optical loop mirror," *J. Lightwave Technol.*, vol. 18, pp. 1001–1006, July 2000.
- [22] —, "All optical wavelength conversion of short pulses and NRZ signals based on nonlinear optical loop mirror," *J. Lightwave Technol.*, vol. 18, pp. 1007–1013, July 2000.
- [23] J. P. R. Lacey, M. A. Summerfield, and S. J. Madden, "Tunability of polarization insensitive wavelength converters based on four wave mixing in semiconductor optical amplifiers," *J. Lightwave Technol.*, vol. 16, pp. 2419–2427, Dec. 1998.
- [24] S. Yamashita, S. Y. Set, and R. I. Lamming, "Polarization independent, all fiber phase conjugation incorporating inline fiber DFB lasers," *IEEE Photon. Technol. Lett.*, vol. 10, pp. 1407–1409, Oct. 1998.
- [25] K. Inoue, M. Yoshino, and F. Kano, "Polarization insensitive wavelength conversion using a light injected DFB-LD with loop configuration," *Electron. Lett.*, vol. 30, no. 5, pp. 438–439, 1994.
- [26] M. Yoshino and K. Inoue, "Polarization insensitive LD wavelength conversion using a loop configuration with a filtering function," *Electron. Lett.*, vol. 32, no. 18, pp. 1699–1700, 1996.
- [27] G. A. Nowak, Y.-H. Kao, T. J. Xia, M. N. Islam, and D. Nolan, "Low-power high-efficiency wavelength conversion based on modulational instability in high-nonlinearity fiber," *Opt. Lett.*, vol. 23, no. 12, pp. 936–938, 1998.
- [28] S. Y. Set, H. Geiger, R. I. Laming, M. J. Cole, and L. Reekie, "Optimization of DSF and SOA based phase conjugators by incorporating noise-suppressing fiber gratings," *IEEE J. Quantum Electron.*, vol. 33, pp. 1694–1698, July 1997.
- [29] K. Inoue, "Experimental study on channel crosstalk due to fiber four-wave mixing around the zero dispersion wavelength," *J. Lightwave Technol.*, vol. 12, pp. 1023–1028, June 1994.
- [30] G. P. Agrawal, *Nonlinear Fiber Optics*, 2nd ed. New York: Academic, 1995.
- [31] D. Derickson, *Fiber Optic Test and Measurement*. Englewood, NJ: Prentice-Hall, 1998.
- [32] X. Zhang and B. F. Jergensen, "Noise characteristics and optimum fiber length of spectral inversion using four-wave mixing in a dispersion shifted fiber," *Opt. Fiber Technol.*, vol. 3, no. 1, pp. 28–43, 1997.
- [33] P. O. Hedekvist and P. A. Andrekson, "Noise characteristics of fiber based optical phase conjugators," *J. Lightwave Technol.*, vol. 17, pp. 74–79, Jan. 1999.
- [34] C. R. S. Fludger, V. Handerek, and R. J. Mears, "Pump to signal RIN transfer in Raman fiber amplifiers," *J. Lightwave Technol.*, vol. 19, pp. 1140–1148, Aug. 2001.



Mohammed N. Islam received the B.S., M.S., and Sc.D. degrees in electrical engineering from the Massachusetts Institute of Technology, Cambridge, MA, in 1981, 1983 and 1985, respectively.

From 1985 to 1992, he was a member of the technical staff in the photonic switching department and then the advanced photonics department at AT&T Bell Laboratories, Holmdel, NJ. In 1992, he joined the EECS department at the University of Michigan, Ann Arbor, MI, where he is currently a full tenured professor. In 1999, he went on sabbatical leave at Stanford University, and during the 2000 and 2001 academic years was on leave-of-absence at Xtera Communications, Inc. He was a Fannie and John Hertz Fellow from 1981–1985, and in 1992 he was awarded the OSA Adolf Lomb Medal for pioneering contributions to nonlinear optical phenomena and all-optical switching in optical fibers. He also received the University of Michigan research excellence award in 1997 and became a Fellow of the Optical Society of America in 1998. He has published over 100 papers in refereed journals and holds over 75 patents awarded or pending. He has also authored one book, edited a second book, and written numerous book chapters. In addition, he has founded several start-up companies based on his research at the University of Michigan. AccuPhotonics, Inc. was started in 1994, which designed and manufactured fiber-optic probes for biomedical imaging. AccuPhotonics was acquired by Seafloater Associates in 1997. Then, in 1998, he founded Xtera Communications, Inc., which provides long-haul fiber-optic systems based on its unique all-Raman amplification technology. He remains the Chief Technology Officer of Xtera. In 2000, he also founded Optical Regen, Inc., and Cheetah Optics, Inc. Optical Regen designed all-optical regeneration equipment for long-haul fiber-optic systems, while Cheetah Optics designed tunable filters and ADD-DROP multiplexers for dynamic fiber-optic networks. Both new companies have been acquired and merged into Xtera Communications.

Özdal Boyraz (S'02) received the B.S. degree in electrical engineering from the Hacettepe University, Turkey, in 1993, and the M.S. and Ph.D. degrees in electrical engineering from the University of Michigan, Ann Arbor, MI, in 1997 and 2001, respectively.

He is currently with Xtera Communications, Allen, TX, working on the development of high-capacity long-haul transmission systems. His research includes linear and nonlinear aspects of fiber-optics communications systems, all-optical switching and access node design, optical dense wavelength-division-multiplexing (DWDM) sources, and optical amplifiers. He has been awarded with full scholarship by the Turkish government for his graduate studies.